



6-3-5

NUMERICAL MODELS FOR SIMULATING THE CYCLIC BEHAVIOR AND THE SEISMIC RESPONSE OF STEEL STRUCTURES

Giulio BALLIO , Carlo A. CASTIGLIONI and Federico PEROTTI

Department of Structural Engineering, Politecnico di Milano,
Milano, Italy

SUMMARY

Numerical models are set up for the simulation of the cyclic behavior of cantilevered columns and of concentric cross bracings. These models take into account the Bauschinger effect as well as global and local buckling of the members and low cycle fatigue. For both structural typologies a comparison is presented between numerical and experimental results, both in terms of global appearance of the hysteresis loops and of absorbed energy.

INTRODUCTION

Most of the recent Recommendations dealing with the design of structures in seismic regions (Refs. 1,2) encompass the adoption of a behavior factor (q) for reducing the horizontal forces obtained through a linear analysis, in order to account for the post elastic behavior of the structure.

Among the various parameters influencing the q -factor, a major role is played by the ductility of the structural members, which is, particularly in the case of steel structures, influenced by the hysteretic behavior of the material, by local and global buckling and low cycle fatigue effects. Furthermore, a rational definition of the q -factor must keep into account both the ductility demand connected with the seismic actions and the global inelastic resources of the structure which are influenced for example by the structural typology, the geometric effects due to vertical loads and by brittle fracture mechanisms.

Of course it is not feasible to try to define the behavior factor by means of extensive dynamic testing programs on full scale structures, because of the costs imposed by this kind of approach. A valid alternative is however represented by quasi-static cyclic tests performed on structural elements (or structural systems) combined with numerical simulations of their dynamic behavior.

This second approach can be summarized in the following steps:

- a) define, for a given structural typology under seismic loading, the elements which are deemed to be "critical", in that are supposed to undergo the largest inelastic deformations;
- b) perform quasi-static cyclic loading on such elements;
- c) on the basis of the experimental results obtained at step b) set up numerical models for simulating the behavior of the "critical" elements;

- d) analyze the test results b) and define appropriate collapse criteria and characteristic damage indexes for these elements;
- e) perform dynamic nonlinear numerical simulations by means of the models previously set up and calibrated and rielaborate the results on the basis of the adopted collapse criteria.

Following this philosophy, at the Structural Engineering Department of Politecnico di Milano, some cyclic test were performed on concentric truss bracings and cantilevered columns, and numerical models were set up for simulating the behavior of both these structural typologies. In this paper the numerical models are briefly described and the results are compared with the experimental ones.

NUMERICAL MODELS

Cantilevered Columns The model adopted for simulating the behavior of columns under compression and bending consists of a rigid bar connected to the ground by a "cell" where all the deformability of the member is concentrated (Refs. 3,4) and a structural mass applied on the top. The behavior of the "cell" follows a constitutive law for the material and some rules related to a damage model.

Concentric Cross Bracings The model adopted in the simulation of concentric cross bracing systems consists of a pin-ended rigid frame with two diagonal bars connected at the intersection point. Each diagonal is modelled (Refs. 5,6) as two rigid members connected by a deformable cell that behaves depending on a damage model and a constitutive law for the material similar to those set up for the cantilevered columns. Furthermore, the model accounts for bolted joints slippage. Structural masses are considered applied at the top of the frame structure.

THE CONSTITUTIVE LAW OF THE MATERIAL

It is supposed that the structural steel behaves, under cyclic loading, following the equation proposed in (Ref.7) :

$$\sigma^* = \alpha \epsilon^* + (1 - \alpha) \epsilon^* / [1 + |\epsilon^*|^{R(\zeta)}]^{1/R(\zeta)} \quad (1)$$

with $R(\zeta) = R_0 - f(\zeta)$ a decreasing function of the plastic strain at the previous cycle. In equation (1) σ^* and ϵ^* are non dimensional values of the current stress and strain in the branch of the hysteresis loop under consideration, while exponent R is a parameter governing the shape of the transition curve between the initial slope and the yield asymptote inclined by α (Ref. 8).

In order to account for the effects of random loading, a set of rules is introduced, extending the validity of the model, although limiting the amount of memory required to keep into account the past stress-strain history. As proposed by Filippou, Bertero and Popov (Ref. 9), only four controlling curves are memorized and considered at each step:

- a) the monotonic envelope
- b) the ascending upper branch curve, originating at the reversal point with the smallest ϵ value
- c) the descending lower branch curve, originating at the reversal point with the largest ϵ value
- d) the current curve, originating at the most recent reversal point.

Furthermore, in order to keep into account the isotropic hardening, the yield asymptote is shifted before computing the new asymptote intersection point following the strain reversal, as proposed by Stanton and McNiven (Ref. 10). The stress shift of the asymptote is assumed to depend on the maximum plastic strain at the instant of strain reversal.

MODELLING THE STRUCTURAL DAMAGE

In order to model its behavior, the cross section is divided into a finite number of strips, each one characterized by area, distance from the center of gravity, residual stresses, yield stress and by some constants related to the damage process. In fact, it is supposed that, under cyclic loading, structural damage can develop in each strip, due to the following effects:

- a) Local buckling
- b) Low cycle fatigue
- c) Fracture

It is assumed that, for the single strip, the collapse caused by each one of the previous effects (considered separately) is governed by a single parameter. It is then possible to define three indexes of partial damage, I_{LB} , I_{LCF} and I_F each given by the ratio of the current value of a suitable deformation parameter to a significant value related to each physical phenomenon, that is:

- a) Euler strain for local buckling,
- b) ultimate tensile strain for fracture,
- c) absorbed energy (computed on the basis of number of cycles and plastic strain) for low-cycle fatigue.

An "effective" damage index I_{ED} is then defined for the strip, by properly combining the partial damage indexes: $I_{ED} = \sqrt{(\beta I_{LB}^2 + \gamma I_{LCF}^2 + \delta I_F^2)}$, with β, γ and δ combination coefficients ≤ 1 (Ref. 4).

The damage process is simulated by reducing the area of each strip according to: $A_1 = A_0(1 - I_{ED})$. Of course $I_{ED} = 1$ corresponds to the collapse of the strip which is definitively cancelled. The weight coefficients β, γ and δ were calibrated in order to obtain the best fit of the experimental results.

It was found (Ref. 4) that, for a given section shape (e.g. IPE or HE), their values remain practically constant, independently, for example, on loading history and specimen size.

RESULTS

Tests were performed on both cantilevered columns and concentric cross-bracing systems at the Structural Engineering Department testing facilities of Politecnico di Milano. The testing machine allowed to impose quasi-static displacements to the specimens. When choosing the loading history, reference was made to the testing procedures proposed by ECCS (Ref. 11). In order to evaluate the influence of isotropic hardening, variable amplitude loading and displacement range, both displacement histories symmetric and non-symmetric with respect to the origin were adopted.

Cantilevered Columns A first series of tests were performed on welded steel box and I shapes, with high local slenderness ratios (b/t) of the plates (Ref. 3), while a second series of tests were performed on rolled I shapes of the commercial series IPE and HE (Ref. 4). In this paper some results are presented relative to an IPE 300 profile, with flange plates 150 mm wide and 10.7 mm thick

($b/t=14$), and to a HEA 220 profile with flange plates 220 mm wide and 11 mm thick ($b/t=20$). Fig. 1(a) shows the horizontal top load - displacement plot of the test performed on a IPE 300. The numerical simulation results are plotted in fig. 1(b). Figs. 2(a) and 2(b) show respectively the experimental and the numerical simulation plots in the case of a HEA 220 profile. The tests were carried out with different displacements histories. In both cases, the numerical model is capable to interpret the behavior of the real member fairly well, showing a gradual reduction in both stiffness and resistance in good agreement with those shown by the tested members. The good agreement between the numerical model and the experimental results is also evident when examining the following figs. 3 and 4, where, for all the tests performed on IPE 300 and HEA 220 shapes, the ratios of the numerical to the experimental total absorbed energy are plotted against the cycle amplitude, normalized on the limit elastic displacement. It can be noticed that for both shapes, the disagreement is usually of the order of magnitude of the 10%.

Concentric Cross Bracings A series of test were performed on concentric cross bracing systems, with both one or two diagonal members (Ref. 6). The diagonals' cross-section was built up by either two angles or two channels shapes. All these tests were carried out imposing displacements histories simmetric with respect to the origin. Fig. 5(a) shows the horizontal top force-displacement plot of the test on a single diagonal built up by two channels C80. For comparison, fig. 5(b) shows the numerical simulation output. The same comparison between experimental and numerical results is presented in figs. 6(a) and 6(b) respectively, in the case of a bracing system with two diagonal members. The cross section is built up by two channels C80. In both cases it is evident that the numerical model interprets fairly well the structural behavior of the bracing system, in particular the gradual deterioration due to local buckling problems and the typical slippage of the bolted joints. In the following fig. 7, the ratios of the numerical to the experimental total absorbed energy are plotted against the cycle amplitude, normalized on the limit elastic displacement for the two previous example, and for a cross bracing system with two diagonal members built up by two angles 50 x 6. It can be noticed that, independently on the geometry of the bracing and on the adopted shapes the numerical model can interpret the energy dissipation of the real structure with deviations usually smaller than 10%.

CONCLUSIONS

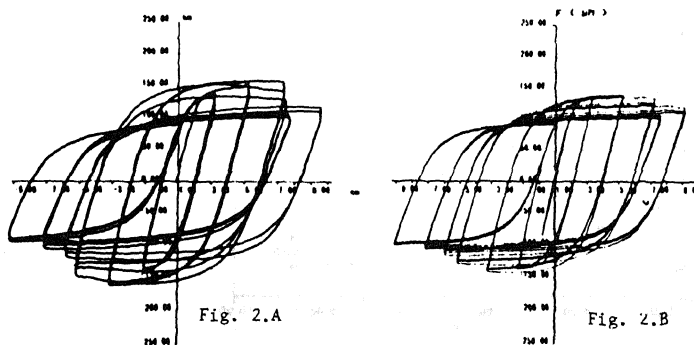
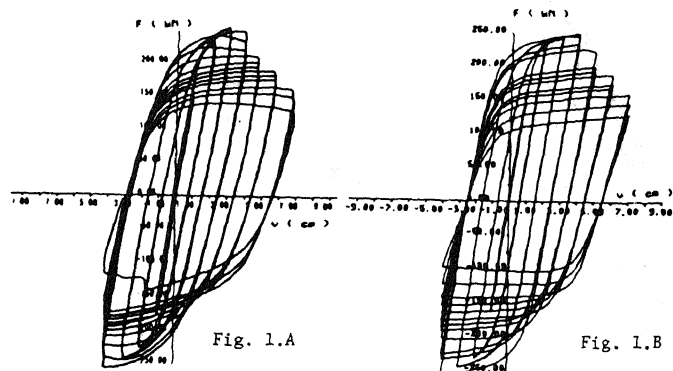
A numerical method was set up which allows the simulation of the behavior of concentric bracing systems and cantilevered columns under cyclic loads. This model accounts for the non linear behavior of the material, the Bauschinger effect and damage caused by local and global buckling, fatigue and fracture. The results show that the energy absorbed by the real structure and that computed by the model differ for no more than the 10%.

The model may be useful either for simulating a very large number of quasi-static tests aimed to the calibration of simpler hysteretic models to be used in the dynamic analysis of large structural systems or directly for the dynamic simulation of the behavior of simple structures (Ref. 12).

REFERENCES

1. Eurocode-8, "European Code for Seismic Regions" (1988).
2. Seismology Committee, Structural Engineers Association of California, "Tentative Lateral Forces Requirements", (1985).
3. Ballio, G. and Calado, L., Steel Bent Sections under Cyclic Loads. Experimental and Numerical Approaches", Costruzioni Metalliche, 1, (1986).

4. Castiglioni, C.A. and Di Palma, N., "On the Behavior of Steel Members under Cyclic Loading: Testing and Numerical Simulation", Structural Engineering Dept., Politecnico di Milano, Technical Rept., to be published.
5. Ballio, G. and Perotti, F., "A Finite Element Describing Axially loaded Members Subjected to Cyclic Loads", Proc. of the Euromech Colloquium No. 174, "Inelastic Structures Under Variable Loads", Palermo, (1983).
6. Ballio, G. and Perotti, F., "Cyclic Behavior of Axially loaded Members: Numerical Simulation and Experimental Verification", Journal of Constructional Steel Research, 7, (1987)
7. Menegotto, M. and Pinto, P.E., "Method of Analysis for Cyclically Loaded Reinforced Concrete Plane Frames Including Changes in Geometry and Nonelastic Behavior of Elements under Combined Normal Force and Bending", Proc. IABSE Symposium on the Resistance and Ultimate Deformability of Structures Acted on by Well Repeated Loads, Lisbon, (1973).
8. Castiglioni, C.A., "Numerical Simulation of Steel Shapes under Cyclic Bending: Effect of the Constitutive Law of the Material", Costruzioni Metalliche, 3, (1987).
9. Filippou, F.C., Bertero, V.V. and Popov, E.P., "Effects of Bounds Deterioration on Hysteretic Behavior of Reinforced Concrete Joints", Earthquake Engineering Research Center Report UCB/EERC-83/19, University of California, Berkeley, (1983)
10. Stanton, J.F. and McNiven, M.D., "The Development of a Mathematical Model to predict the Flexural Response of Reinforced Concrete Beams to Cyclic Loads Using System Identification", Earthquake Engineering Research Center Report UCB/EERC-79-02, University of California, Berkeley, (1979).
11. ECCS-TWG 1.3, "Study on the Design of Steel Buildings in Earthquake Zones", (1985).
12. Ballio, G., Castiglioni, C.A. and Perotti, F., "On the Assessment of Structural Design Factors for Steel Structures", 9th World Conference on Earthquake Engineering, Tokyo, (1988).



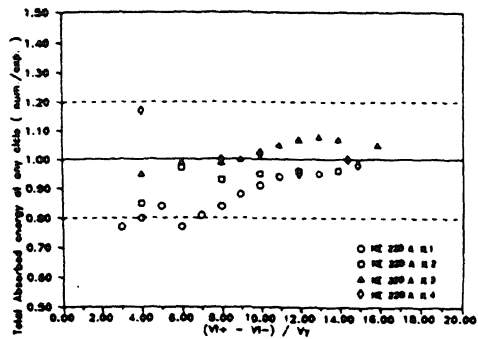


Fig. 3

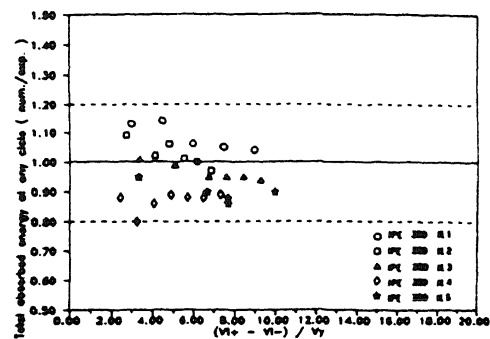


Fig. 4

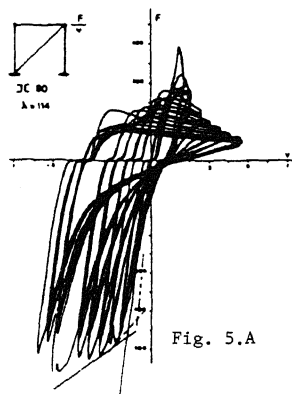


Fig. 5.A

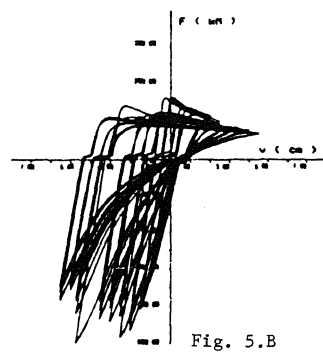


Fig. 5.B

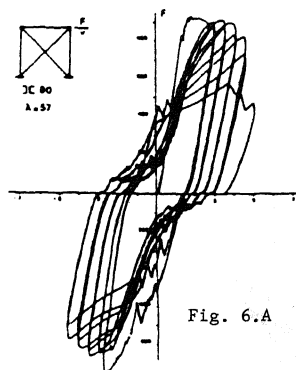


Fig. 6.A

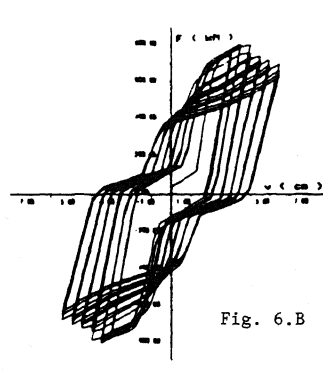


Fig. 6.B

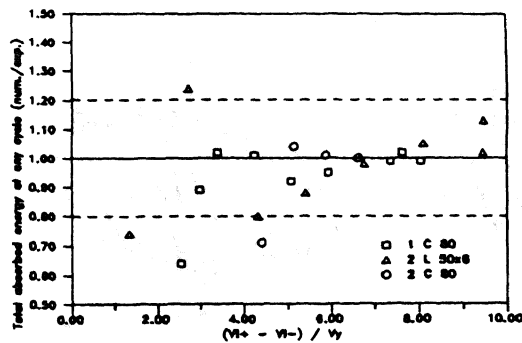


Fig. 7